



## 3D graphene based materials for energy storage



Xueliu Fan<sup>a</sup>, Xuli Chen<sup>a</sup>, Liming Dai<sup>a,b,\*</sup>

<sup>a</sup> Department of Macromolecular Science and Engineering, Case Western Reserve University, 10900 Euclid Avenue, Cleveland, OH 44106, United States

<sup>b</sup> Center of Advanced Science and Engineering for Carbon (Case4Carbon), Case Western Reserve University, 10900 Euclid Avenue, Cleveland, OH 44106, United States

### ARTICLE INFO

#### Article history:

Received 12 October 2015

Accepted 7 November 2015

Available online 20 November 2015

#### Keywords:

3D graphene  
Supercapacitor  
Battery  
Energy storage

### ABSTRACT

Three-dimensional graphene based materials have attracted great attention as they not only possess the intrinsic properties of graphene, but also provide high specific surface area, low density, good electrical conductivity, and excellent mechanical properties. As a consequence, three-dimensional graphene materials have been extensively studied for various potential applications, including supercapacitors and batteries for energy storage. Here, we present a focused review on recent progresses and challenges in the synthesis of three-dimensional graphene materials and their applications in energy storage devices.

© 2015 Elsevier Ltd. All rights reserved.

### 1. Introduction

In the twenty-first century, one of the great challenges is the rapid increase in global energy consumption while the reserve of fossil fuels in the nature is limited. Thus, it is critically important to develop new and eco-friendly energy conversion and storage systems based on innovative materials [1]. In this context, electrode materials with a high electrical conductivity, large surface area, ease of functionalization, and excellent electrochemical properties are highly desirable [2]. Because of their special physicochemical structures and excellent electrochemical properties, carbon nanomaterials (e.g., carbon nanotubes (CNTs), graphene) have been widely studied for applications in electrochemical energy storage systems, including supercapacitors and batteries [1].

Graphene is a monolayer of carbon atoms packed into honeycomb lattice [3,4]. Since Novoselov and coworkers isolated single layer graphene by mechanical cleavage from graphite in 2004 [5], graphene has attracted great attention [6]. Due to its unique structure, graphene possesses extraordinary physicochemical properties, such as high carrier mobility [7], high thermal conductivity [8], and promising elasticity and stiffness [9]. During the past decade, various methods have been developed to synthesize graphene, including bottom-up approaches (e.g., epitaxial growth [10,11], chemical vapor deposition (CVD) [12–14]) and top-down approaches (e.g., chemical or ultrasonic exfoliation of graphite [15,16]). Among many potential applications, two-dimensional (2D) graphene sheets have been widely studied as electrode materials in energy storage devices, particularly supercapacitors [17,18] and batteries [19,20].

To further enhance the performance of graphene electrodes, three-dimensional (3D) architectures of graphene (e.g., foam, network, gels) have been recently developed [21]. These 3D graphene-based materials not only possess the intrinsic properties of graphene, but also provide a high specific surface area, low density, good mechanical strength, and excellent electrical conductivity [22]. In this article, we will provide a focused review on the preparation of 3D graphene-based electrode materials for energy storage applications.

### 2. 3D graphene-based nanomaterials

#### 2.1. Synthesis and structure of 3D graphene nanomaterials

As shown in Fig. 1, the porous structure is a common characteristic of 3D graphene nanomaterials, including graphene foams, networks, gels, and graphene-CNT hybrid structures. In particular, graphene foams can be synthesized by CVD method on nickel foams as the template (Fig. 1a–f) [23]. After removal of the nickel foam template, the porous structure can be reserved. On the other hand, graphene gels can be synthesized by freeze drying graphene oxide, with or without reduction, leading to a crosslinked graphene hydrogel or aerogel (Fig. 1g–i) [24]. The recently reported graphene-CNT integrated 3D materials with a pillared structure can be produced by one or multiple-step CVD processes (Fig. 1j–m) [25,26]. Having tunable micro, meso, and macro porous structures, these 3D graphene nanomaterials possess extraordinary surface, mechanical, and electrical and electrochemical properties.

Table 1 summarizes the main synthesis methods to produce 3D graphene architectures, along with some of the unique properties and applications. In the following sections, we will provide more details on the synthesis of various 3D graphene based materials.

\* Corresponding author.

E-mail addresses: [xxf53@case.edu](mailto:xxf53@case.edu) (X. Fan), [xxc240@case.edu](mailto:xxc240@case.edu) (X. Chen), [lxid115@case.edu](mailto:lxid115@case.edu) (L. Dai).

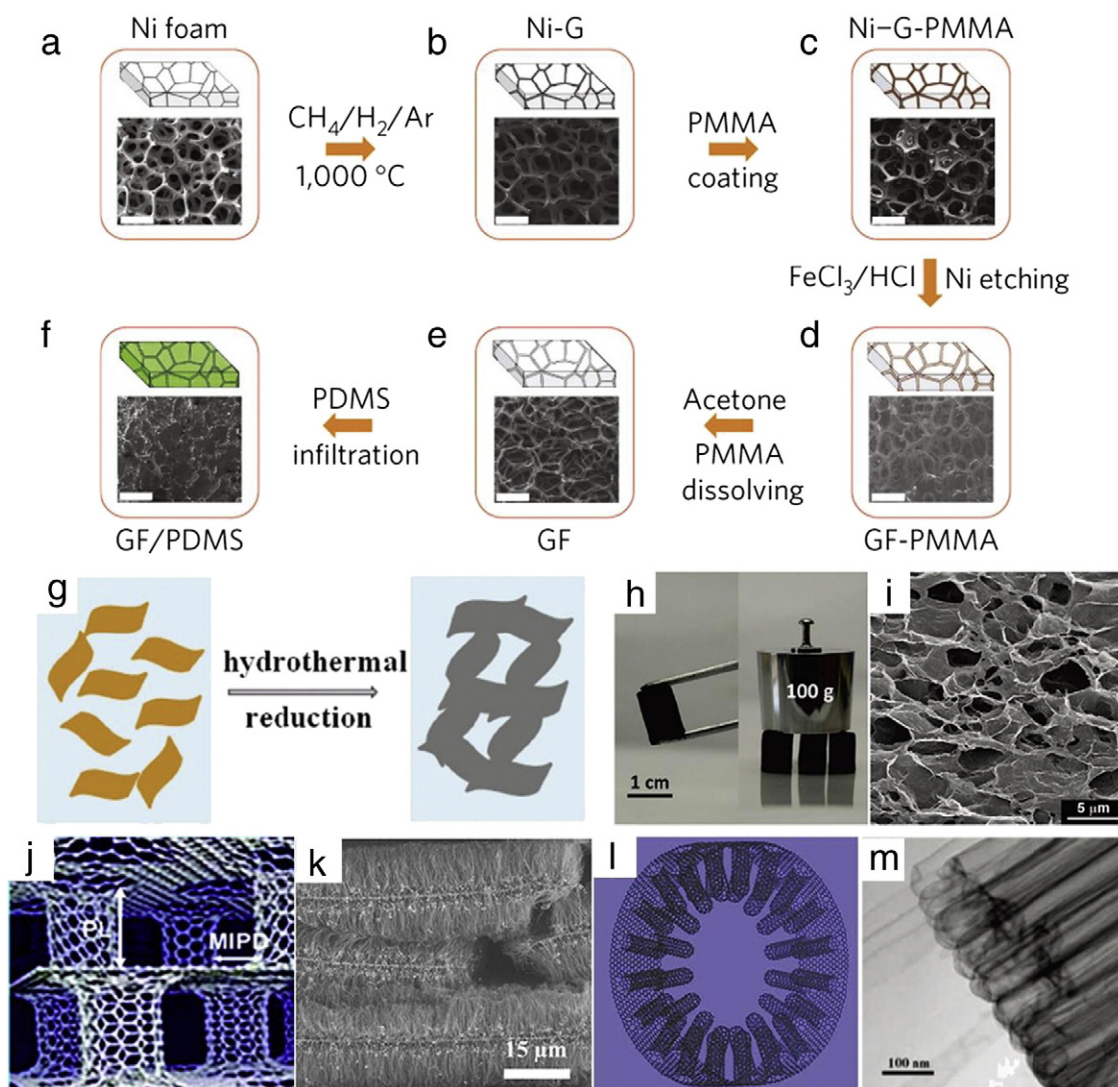


**Fig. 1.** (a–f) Synthesis of the 3D graphene foam by template-assisted synthesis and its integration with polydimethylsiloxane (PDMS) [23']. (Reprinted from Ref. [23'] with permission. Copyright 2011, Macmillan Publishers Ltd) (g) Schematic illustration of the self-assembled graphene hydrogel (SGH) formation mechanism. (h) Optical image of the SGH with ability of easy handling and supporting weight; (i) SEM image of the SGH microstructure [24']. (Reprinted from Ref. [24'] with permission. Copyright 2010, American Chemical Society). (j) Schematic illustration and (k) typical SEM image of the 3D pillared graphene/CNT nanostructure [25]. (Reprinted from Ref. [25] with permission. Copyright 2011, American Chemical Society) (l) Schematic illustration and (m) TEM image of the 3D graphene-radially aligned CNT structures with closed end of radially aligned CNTs [26']. (Reprinted from Ref. [26'] with permission. Copyright 2015, American Advanced Association for Science).

### 2.1.1. CVD derived 3D graphene nanomaterials

Bottom-up approach has played an important role in developing controlled fabrication of desired 3D graphene architectures. The most commonly used bottom-up approach is CVD, which can lead to high-quality monolayer/few layers of graphene. During the synthesis, carbon atoms are directly deposit on a desired network support/template, which also acts as the catalyst required for the formation of graphene layer(s) in the 3D architecture.

Chen et al. used nickel or copper foams as templates to grow 3D graphene foams with interconnected network structures [23'] (Fig. 1a–f). The resultant free-standing graphene foams were demonstrated to show an ultralow density of  $5 \text{ mg/cm}^3$  and high specific surface area of  $\sim 850 \text{ m}^2/\text{g}$ , being one of the lightest aerogels. Raman spectra of the 3D graphene foams showed a distinct G band at  $\sim 1528 \text{ cm}^{-1}$  characteristic of the  $\text{sp}^2$  carbon and a negligible disorder-induced D peak at  $\sim 1345 \text{ cm}^{-1}$ , indicating a high graphitization degree [39]. Consequently, these graphene foams exhibited a high electrical conductivity of  $\sim 10 \text{ S/cm}$ , a value which is  $\sim 6$  order of magnitude higher than that of the chemically derived graphene [1]. In addition to the

metal substrate, ceramic templates have also been used for the CVD growth of 3D graphene materials. For instance, Ning et al. used a porous MgO template for thermal pyrolysis of methane ( $\text{CH}_4$ ) to produce graphene nanomeshes with a specific surface area as high as  $1654 \text{ m}^2/\text{g}$  [31]. In a similar but independent study, Zhou et al. used porous  $\text{Al}_2\text{O}_3$  ceramics as templates to produce graphene tubes and porous graphene/ $\text{Al}_2\text{O}_3$  composites with a sheet electrical resistance as low as  $0.11 \text{ } \Omega/\text{sq}$  and thermal conductivity of  $8.28 \text{ W}/(\text{m} \cdot \text{K})$  [40].

These highly conductive 3D graphene architectures can serve as ideal scaffolds and backbones for depositing inorganic materials (e.g.,  $\text{Fe}_3\text{O}_4$  [41,42],  $\text{Co}_3\text{O}_4$  nanowires [43], NiO [44], ZnO [42],  $\text{MnO}_2$  [29]) and organic materials (e.g., polyaniline (PANI) [45]) to be used as high-performance electrodes in supercapacitors and batteries. Furthermore, doping these graphene foam electrodes with heteroatoms (e.g., N, B, P) can enhance their electrical conductivity and surface hydrophilicity [46–48].

An alternative route for effective synthesis of 3D graphene materials is to use polymer precursors. Since Sun et al. reported the synthesis of graphene by pyrolysis of poly(methyl methacrylate) (PMMA) precursor

**Table 1**  
Summary of main methods to synthesize 3D graphene based nanomaterials for energy storage applications.

Prepared method	3D graphene sample	Properties	Device	Ref
CVD on nickel foam	Graphene foam	Specific surface area ~850 m <sup>2</sup> /g, ultralow density of ~5 mg/cm <sup>3</sup> , high porosity of ~99.7%, high electrical conductivity ~10 S/cm, the resistance only increases ~2.7% after 10,000 cycles' bending	Lithium-ion batteries	[23',27]
CVD on nickel foam and nitrogen doping	N-doped graphene foam	Specific surface area ~357 m <sup>2</sup> /g, enhanced thermal stability with a decompression temperature of 584 °C for N-doped graphene foam	Sodium-ion batteries	[28]
CVD on nickel foam and electrochemical deposition	Graphene foam/MnO <sub>2</sub>	Surface area ~392 m <sup>2</sup> /g, lightweight density 0.75 mg/cm <sup>2</sup> , electrical conductivity ~55 S/cm	Supercapacitor	[29]
CVD on colloidal silica	Graphene network	Specific surface area ~1025 m <sup>2</sup> /g, electrical conductivity ~52 S/cm	Double-layer capacitor	[30]
CVD on porous MgO layers	Graphene nanomesh	Large specific surface area ~1654 m <sup>2</sup> /g, unchanged specific surface area after calcination at up to 1000 °C	Supercapacitor	[31]
CVD via seamless growth of CNT on graphene	Covalently bonded graphene/CNT hybrid material	High specific surface area 2000–2600 m <sup>2</sup> /g	Supercapacitor	[32]
Hydrothermal process Freeze drying	Graphene hydrogel	2.6% graphene sheets electrical conductivity ~5 × 10 <sup>-3</sup> S/cm, storage modulus ~470 kPa, yield stress ~11.7 kPa	Supercapacitor	[24']
Hydrothermal process and electrodeposition	Polypyrrole (PPy)-graphene foam	Specific surface area ~463 m <sup>2</sup> /g, highly reversible and durable foam behavior after compression at the maximum strain (ε = 50%) for 1000 cycles	Supercapacitor	[33']
Hydrothermal process Freeze drying	N and B Co-doped graphene aerogel	Specific surface area ~249 m <sup>2</sup> /g for BN-graphene aerogel	Supercapacitor	[34]
Chemical reduction freeze drying	Fe <sub>3</sub> O <sub>4</sub> /graphene aerogel	Specific surface area ~96 m <sup>2</sup> /g, pore size 2–100 nm, pore volume 0.28 cm <sup>3</sup> /g, electrical conductivity ~15 S/cm	Lithium-ion batteries	[35]
Chemical reduction Filtration	Macroporous graphene frameworks	Specific surface area ~194 m <sup>2</sup> /g, electrical conductivity ~1024 S/cm	Supercapacitor	[36]
Chemical reduction	Graphene/CNTcomposites	Specific surface area ~539 m <sup>2</sup> /g	Supercapacitor	[37]
Hydrothermal process Solvent-exchange approach	Solvated graphene frameworks (SGF)	Largely maintained solvated porous network after pressing a high electrical conductivity of ~950 S/m in the pressed SGF film	Lithium-ion batteries	[38]

on a Cu substrate [49'], 3D graphene nanomaterials have been prepared by pyrolysis of polymer–3D template mixtures or polymer coated onto 3D templates with pore sizes down to micro and nano scales [30,50]. Of particular interest, Yoon et al. synthesized 3D graphene nano-networks with a specific surface area of 1025 m<sup>2</sup>/g and conductivity of 52 S/cm, which are much higher than those of traditional 3D graphene materials [30]. In this particular study, a solution of poly(vinyl alcohol) (PVA)-FeCl<sub>3</sub> was infiltrated into a self-assembled nanometer-scaled colloidal silicon template, and annealed at 1000 °C under hydrogen atmosphere to produce the 3D graphene nano-network.

Although the synthesis of 3D graphene nanomaterials on the network catalytic substrates by CVD is a scalable process, the substrate removal is tedious and often introduces contaminants that may hinder applications of the resultant 3D graphene materials. To address this issue, plasma enhanced CVD (PECVD) has been developed to grow 3D graphene without catalyst [51–53]. Through plasma deposition of gas precursors (e.g., methane or acetylene) under hydrogen and argon atmosphere, Yang et al. have produced 3D graphene walls on a SiO<sub>2</sub> wafer and other dielectric substrate without the involvement of any catalyst [51].

### 2.1.2. Self-assembled 3D graphene from GO reduction

Graphene oxide (GO), containing epoxy and hydroxyl groups on the basal plane and carbonyl and carboxyl groups at the edge [15,54], is usually prepared by oxidizing graphite through the Hummers' method [55"]. Depending on the force balance between their static repulsion from the functional groups and the van der Waals attraction between the basal planes, GO can be gelled and reduced into self-assembled 3D graphene structures [24',54]. Since Li et al. found that uniform graphene gels could be obtained by reducing GO with a relatively low concentration (0.5 mg/mL) [56], considerable efforts have been devoted to the preparation and optimization of self-assembled 3D graphene via GO reduction [57]. Since the preparation of 3D graphene architectures from reduction of GO has been summarized in several comprehensive reviews [57–59], we will give a brief focused overview of the work related to energy storage below.

One of the simplest, but efficient, methods to produce 3D graphene structures is through in-situ self-assembling of GO during reduction [24',58–60]. The formation of GO gels occurred when the increased van der Waals force between the basal planes during the reduction overbalanced the static repulsion force of functional groups. As a demonstration of this approach, Xu et al. sealed an aqueous dispersion of GO with a concentration of 2 mg/mL in a Teflon-lined autoclave, followed by heating up to 180 °C for 12 h (Fig. 1g), to produce 3D graphene hydrogel containing ~2.6% graphene sheets with a high electrical conductivity of 5000 S/cm [24'] (Fig. 1h and i). On the other hand, Liu and Seo used a vacuum centrifugal evaporation approach to assemble 3D porous GO networks via van der Waals forces, followed by thermal annealing under hydrogen and argon to convert GO into 3D reduced GO (rGO) [61].

Alternatively, 3D graphene architectures can also be obtained by adding cross-linking agents, such as polymers [62], bio-molecules [63, 64], and/or metal ions [65], to enhance the GO gelation. In this regard, Bai et al. have mixed a GO dispersion with a PVA solution to obtain the GO network structure [62], while Xu et al. mixed double-stranded DNA chains with a GO dispersion to form single-stranded DNA chains, which bridged GO sheets to produce 3D GO/DNA hydrogels [63]. Other approaches to 3D GO/graphene structures include electrochemical reduction [66], interferometric lithography [67], template-assisted assembly [36,68], graphene nanoplatelets by ball-milling [69'], graphene papers [70], graphene fabrics [71] grown on the Ni/Cu fabrics, and graphene networks [72] derived from the Cu network template.

### 2.1.3. 3D graphene and CNT hybrids

Two allotropic carbon materials, graphene and CNTs, have been combined to construct 3D architectures, through either multi-step growth with metal catalysts [25,32,37,73–75] or one-step growth without catalyst to form 3D seamless carbon nanomaterials [26']. Graphene-CNT 3D carbon nanomaterials have been proved to exhibit promising electrical and thermal conductivities with a large specific surface area attractive for energy storage [20,74].

For most CVD approaches, catalysts (e.g., Fe and Al<sub>2</sub>O<sub>3</sub>) are usually used for depositing graphene, which is followed by CVD growth of

CNT to form the 3D graphene-CNT hybrid carbon nanomaterials. As reported by Zhu et al. [32], a catalyst layer of 1 nm Fe and 3 nm  $\text{Al}_2\text{O}_3$  was deposited on a preformed graphene sheet for the CVD growth of a CNT carpet under ethylene/acetylene, hydrogen and argon atmosphere at 750 °C. TEM images revealed that the open-ended CNT had the "covalently bonded" with the graphene base around the catalyst residues. The resultant hybrid 3D graphene-CNT carbon nanomaterials exhibited a surface area  $>2000 \text{ m}^2/\text{g}$ , which can be used for microsupercapacitor fabrication by patterning catalyst particles (Fe/ $\text{Al}_2\text{O}_3$ ) [76]. An alternative approach to the 3D graphene-CNT structure has been reported by intercalated growth of vertical-aligned CNTs (VACNTs) into thermally-expanded highly ordered pyrolytic graphite (HOPG) [25]. In this case, the thermally-expanded HOPG was first coated by  $\text{SiO}_2$  derived from silicon tetrachloride ( $\text{SiCl}_4$ ) under hydrogen and argon at 1000–1200 °C. Subsequent pyrolysis of iron phthalocyanine (FePc) at 800–1000 °C led to the deposition of pillared VACNTs between the graphene layers, forming the 3D pillared graphene-VACNT architecture (Fig. 1j and k). Using surface anodized aluminum wires as the template, 3D graphene-CNT hollow fiber architectures with radially-aligned CNTs (RACNTs) seamlessly sheathed by a cylindrical graphene layer have been recently prepared through one-step catalyst-free CVD (Fig. 1l–m) [26]. This work opens up avenues toward 3D graphene-CNT pillared architectures with covalently-bonded seamless pure C–C nodal junctions between the graphene and CNTs even without catalyst residual at the interface.

3D graphene-CNT sandwiched structures have also been produced by adding  $\text{Co}(\text{NO}_3)_2$  and urea into a GO dispersion, followed by reduction under hydrogen and carbon dioxide at 750 °C for simultaneous growth of CNTs [77]. Other 3D graphene-CNT sandwiched structures have even been obtained by self-assembling. For example, Yu and Dai reported graphene-multiwalled CNT (MWNT) hybrid structures produced from self-assembling of poly(ethyleneimine) (PEI)-modified graphene nanosheets with acid-oxidized CNTs [75]. By tuning the pH value, PEI-modified graphene surface was protonated and sequentially attracted the negatively charged MWNTs to self-assemble them into the interconnected 3D structure with nanoscale pores. Recently, You et al. used the hydrothermal self-assembly approach to obtain 3D nitrogen doped graphene-CNT structures [74]. In this particular case, the pristine CNTs were dispersed in a GO solution, followed by dissolving pyrrole monomers. Upon heating the mixture solution in a sealed Teflon-lined autoclave at 180 °C for 12 h, 3D interconnected frameworks were formed due to the cross-linking behavior of polypyrrole generated from thermal polymerization of pyrrole monomers.

A wide range of the synthetic approaches have been developed to integrate 2D graphene layer into the 3D graphene structure. Since the strong van der Waals forces would lead to the  $\pi$ - $\pi$  restacking interactions between the graphene layers and sacrifice of the specific surface area, it is important to address several key factors in order to maximize the specific surface area in the synthesis of 3D graphene. For 3D graphene architectures derived from the CVD method, the porous density and the specific surface area are both determined by the template structure. For the graphene reduced from GO sheets which have been commonly used to produce the porous structure via self-assembling, it is critical to expand the distance between the graphene layers and to avoid the  $\pi$ - $\pi$  restacking. The introduction of polymers, nanoparticles, and/or CNTs as separating materials between graphene layers can efficiently increase the specific surface area and the pore size.

### 3. Applications in energy storage devices

Along with the rapidly increasing energy consumption on the global scale, the demand for efficient energy storage is growing. Owing to their high specific surface area, good electrical and electrochemical properties, excellent chemical stability and mechanical strength, 3D graphene based materials hold promise for applications in energy storage devices.

In the following sections, we will summarize the applications of various 3D graphene based materials in supercapacitors and batteries.

#### 3.1. Supercapacitors

Supercapacitors, also called ultracapacitors, are the energy storage devices based on fast charge storage and high power delivery mechanism [78,79]. Supercapacitors can be classified into electrical double layer capacitors (EDLC), in which electrostatic charges are accumulated at the electrode/electrolyte interfaces, and the pseudocapacitors to store energy by reversible redox reaction on the electrode surface [80,81]. A typical supercapacitor consists of two electrodes, the electrolyte, and the separator (Fig. 2) [83]. The electrodes are particularly crucial to determine power and energy densities of a supercapacitor [82]. The use of 3D graphene combined with other pseudocapacitor materials as the electrodes has led to various high-performance supercapacitors, as seen below.

##### 3.1.1. Graphene foam based electrodes

Graphene foams have been used as the backbone materials for depositing electrochemically active materials, such as transition metal oxides (e.g., NiO [44],  $\text{MnO}_2$  [29],  $\text{Co}_3\text{O}_4$  [43],  $\text{CoMoO}_4$  [84]) and conductive polymers (e.g., PANI [45]), and then used as the electrode in supercapacitors. In this case, the produced capacitance is contributed by both electrical double-layer capacitance from the graphene foam and pseudocapacitance from the metal oxides or conductive polymers. Conductive polymers, which can experience transition between doped and de-doped states, often give much higher pseudocapacitance than electrical double-layer capacitance. Thus, they have been widely incorporated into 3D graphene foams to produce high-performance electrodes for supercapacitors. For example, Dong et al. fabricated a 3D graphene foam/PANI hybrid electrode material for supercapacitors by in-situ polymerization of aniline monomers on a 3D graphene foam [45]. The resultant supercapacitor exhibited a high specific capacitance of  $\sim 346 \text{ F/g}$  and remained stable after 600 cycles in 1 M  $\text{H}_2\text{SO}_4$  aqueous electrolyte. The high specific capacitance was attributed to pseudocapacitance from PANI and the synergic effect between PANI and 3D graphene architecture. Because of its high electron/electrolyte conductivity and chemical stability, 3D graphene played a critical role in improving the rate capability and cyclic stability.

On the other hand, metal oxides usually show high pseudocapacitance because their faradic reaction beyond formation of electrical double-layers during charge–discharge processes. Moreover, they generally exhibit better stability than polymers during cyclic testing. Therefore, they have also been widely incorporated into 3D graphene

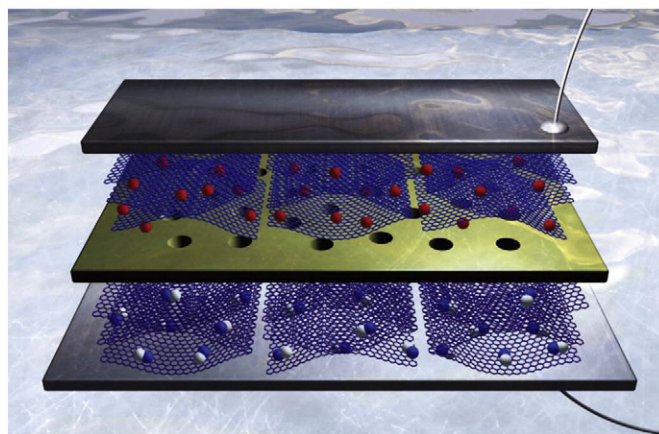


Fig. 2. Supercapacitor device consisting of two graphene electrodes (blue and purple hexagonal planes) and a membrane separator (yellow) [83]. (Reprinted from Ref. [83] with permission. Copyright 2012, Macmillan Publishers Ltd).

materials to improve the performance of supercapacitor electrodes. In this context, Cao et al. fabricated 3D graphene foam via ethanol-CVD by using Ni foam as template [44'] (Fig. 3a). Then, nickel oxide (NiO) was deposited onto the 3D graphene network by potentiostatic electro-deposition. Since CVD-produced graphene foam could avoid restacking of graphene sheets, the electrolyte can readily access through the network. Furthermore, because of the high specific capacitance and well-accepted redox behavior of NiO, the 3D graphene/NiO based supercapacitor exhibited a high specific capacitance of  $\sim 816$  F/g at a scan rate of 5 mV/s in 3 M KOH aqueous electrolyte (Fig. 3b–d). Later, Dong et al. reported even much higher performance of supercapacitors based on 3D graphene foam/cobalt oxide ( $\text{Co}_3\text{O}_4$ ) composite electrodes [43]. The composite was prepared by in-situ growth of  $\text{Co}_3\text{O}_4$  nanowires on a CVD-graphene foam via a hydrothermal method. The resultant 3D graphene/ $\text{Co}_3\text{O}_4$  nanowire based supercapacitor had a high specific capacitance of  $\sim 1100$  F/g at a current density of 10 A/g in 2 M KOH aqueous electrolyte.

### 3.1.2. Self-assembled 3D graphene based electrodes

Self-assembled 3D graphene based materials possess porous structures (e.g., hydrogel [24',86,87], aerogel [34,88,89]) with micro, meso, and macro pores, which are crucial to enhance the performances of the supercapacitor. As Xu et al. reported, the self-assembled graphene exhibited high specific capacitance of 175 F/g in 5 M KOH aqueous electrolyte [24']. Similarly, the performances of the supercapacitors based on the porous graphene structures can be further enhanced by combining with conductive polymers [33',88] or metal oxides [90,91]. Zhao et al. have synthesized 3D graphene/PPy structures by mixing pyrrole monomer with GO by a hydrothermal process, followed by direct electropolymerization of pyrrole and then reduction of GO [33'] (Fig. 4a). Since the pyrrole monomer can  $\pi$ - $\pi$  interact with the GO

sheets, the self-stacking behavior of GO during hydrothermal process can be prevented. The obtained 3D PPy/graphene materials have a specific surface area of  $144$   $\text{m}^2/\text{g}$  and a density of  $40$   $\text{mg}/\text{cm}^3$ , and the 3D graphene/PPy based supercapacitor has the specific capacitance of  $\sim 350$  F/g in 3 M  $\text{NaClO}_4$  aqueous electrolyte (Fig. 4b–d). On the other hand, a specific capacitance of  $310$   $\text{F g}^{-1}$  at 2 mV/s in 1 M  $\text{NaSO}_4$  aqueous solution was reported, in which graphene/ $\text{MnO}_2$  was synthesized by self-limiting deposition of  $\text{MnO}_2$  on the graphene surface using microwave irradiation [90].

### 3.1.3. Graphene-CNT hybrid based electrodes

As mentioned above, graphene-CNT hybrids possess unique advantages as electrode materials for supercapacitors. Yu and Dai developed a poly(ethyleneimine)-modified graphene/MWNT hybrid as the electrode for a supercapacitor, which exhibited a specific capacitance of 120 F/g in 1 M  $\text{H}_2\text{SO}_4$  aqueous solution and could be charged-discharged very fast [75]. On the other hand, Du et al. developed a supercapacitor based on 3D pillared graphene-VACNT hybrid electrodes by intercalated growth of vertically aligned CNT (VACNT) between thermally expanded highly ordered pyrolytic graphite (HOPG), followed by nickel hydroxide coating [25]. The 3D pillared graphene-VACNT based supercapacitor showed a specific capacitance of  $\sim 110$  F/g while the  $\text{Ni}(\text{OH})_2$ -coated graphene-VACNT based-supercapacitor exhibited a high specific capacitance of 1065 F/g with a high rate capability and an excellent cycling ability in 2 M KOH aqueous solution. Similarly, Fan et al. reported a supercapacitor-based 3D graphene-CNT sandwiched structure with CNT pillars grown between graphene layers [77]. The resultant supercapacitor exhibited a specific capacitance of 385 F/g at 10 mV/s in 6 M KOH aqueous solution with good cycling stability. Recently, Lin et al. fabricated a micro-supercapacitor based on 3D graphene-CNT carpets generated by catalyst ( $\text{Fe}/\text{Al}_2\text{O}_3$ ) patterning

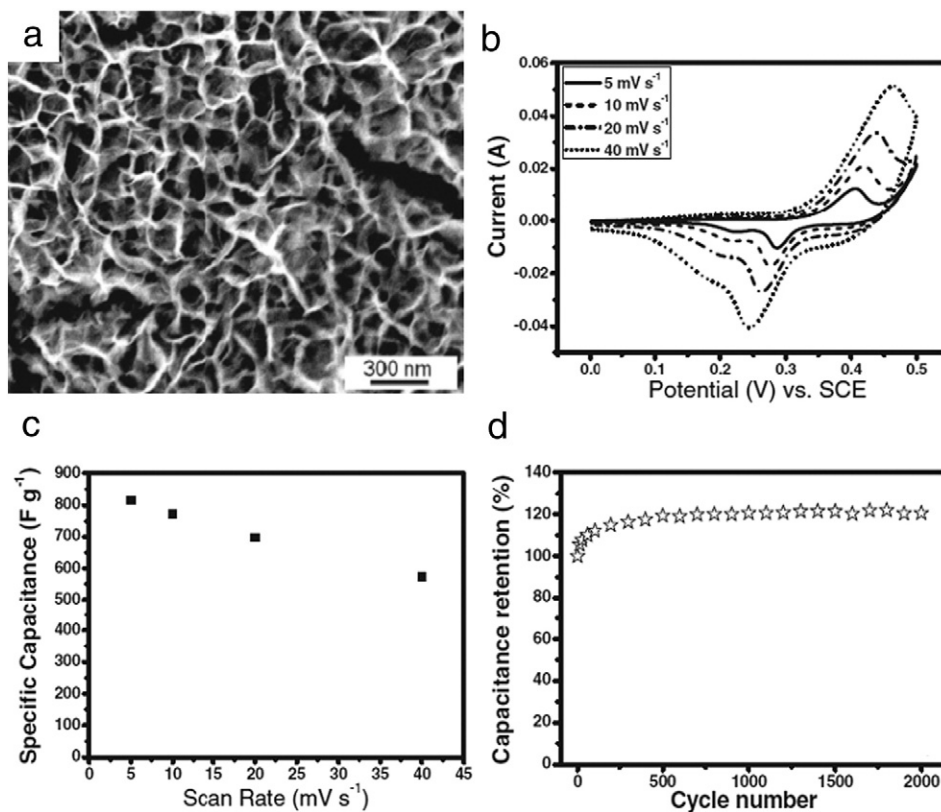


**Fig. 3.** (a) SEM image of 3D graphene/NiO composites. (b) cyclic voltammetry curves measured at scan rates of 5, 10, 20, and 40 mV/s, (c) Specific capacitance dependence on scan rate, (d) cyclic performance of 3D graphene/NiO composites based supercapacitor. [44'] (Reprinted from Ref. [44'] with permission. Copyright 2011, WILEY-VCH Verlag GmbH & Co. KGaA, Weinheim).

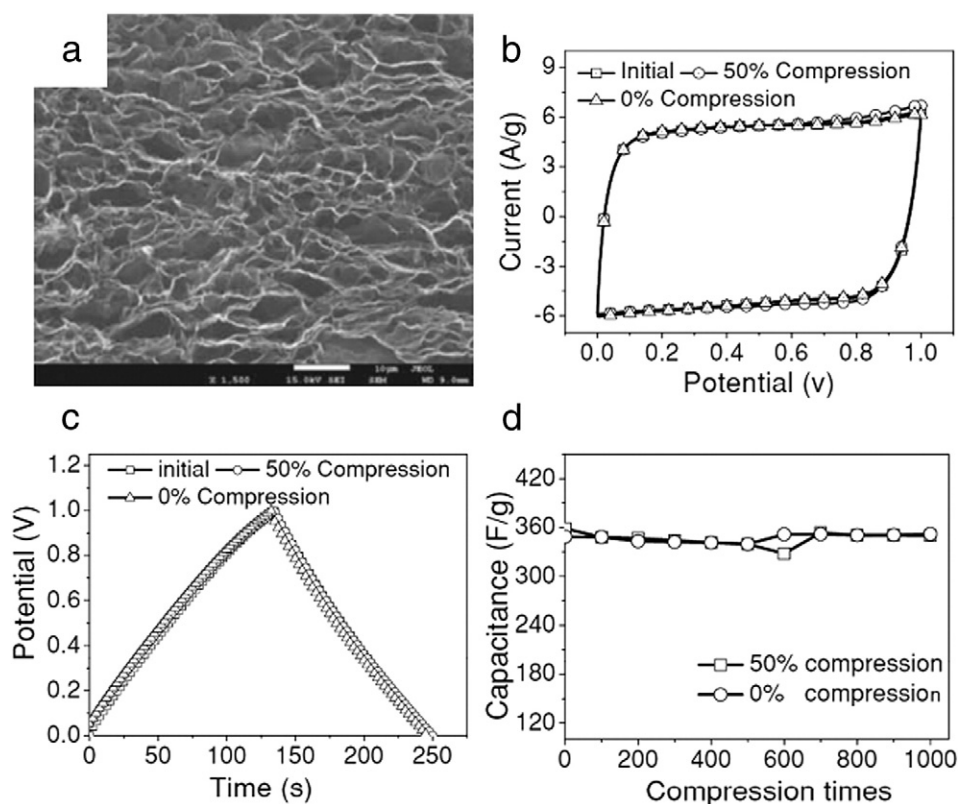


**Fig. 4.** (a) SEM image of the PPy-G foam. (b) CV curves, (c) The corresponding galvanostatic charge–discharge curves, (d) specific capacitances at different compression states for 1000 cycles of the compressible supercapacitor based on PPy-G foam electrodes. [33\*] (Reprinted from Ref. [33\*] with permission. Copyright 2013, John Wiley & Sons, Inc.).

on the graphene, followed by CVD growth of CNTs [76]. The 3D graphene-CNT carpet based supercapacitor thus produced had specific capacitances up to 2.16 mF/cm<sup>2</sup> in aqueous electrolytes and 3.93 mF/cm<sup>2</sup> in ionic liquid. In addition, a high volumetric energy density of 2.42 mWh/cm<sup>3</sup> in the ionic liquid and the power density of 115 W/cm<sup>3</sup> in aqueous electrolyte were achieved.

### 3.2. Lithium-ion batteries

Lithium-ion batteries are the rechargeable power sources that consist of negative electrode (cathode), non-aqueous liquid electrolyte, porous separator, and positive electrode (anode) (Fig. 5) [78,92,93]. During charging, lithium ions move from the cathode to the anode with Li<sup>+</sup> insertion into the anode. Discharge can be completed by the reverse process. Therefore, the anode and the cathode play a crucial role in determining the performance of lithium-ion batteries, including the capacity, the energy density, and the power density. As a traditional anode material, graphite stored lithium through the intercalation of lithium ion into carbon layers with a theoretical specific capacity of 372 mAh/g by forming LiC<sub>6</sub> between two carbon layers [92]. In this case, graphene with single carbon layer structure can store lithium on both sides and thus are supposed to have a much higher theoretical specific capacity [2]. With the high conductivity and large specific surface area, 3D graphene could be an ideal electrode material for lithium-ion batteries.

#### 3.2.1. Anode

3D graphene with pores, holes and a high specific surface area has been demonstrated to offer abundant accessible channels for lithium ion transport [94,95]. Liu et al. synthesized porous graphene paper through freeze-drying homogeneous GO aqueous dispersion into aerogels, followed by mechanical pressing [94]. The lithium-ion batteries based on this porous graphene paper delivered a reversible capacity

of 568 mAh/g at 100 mA/g after 100 charge–discharge cycles. Moreover, 3D graphene with hybrid electroactive materials also greatly improved the cycling performance, which otherwise was rather poor due to the restacking of graphene sheets [79].

On the other hand, concerning the special structure and excellent properties, variety of anode materials, such as transition-metal oxides (e.g., Fe<sub>2</sub>O<sub>3</sub> [96], Fe<sub>3</sub>O<sub>4</sub> [97], TiO<sub>2</sub> [98], MnO<sub>2</sub> [99\*], Mn<sub>3</sub>O<sub>4</sub> [100]), Sn [101], Si [102], chalcogenide [85], halogen elements [69], and CNTs [20,98], have been incorporated with 3D graphene to improve the performance of lithium ion batteries. In this context, Yu et al. fabricated layer-by-layer assembled graphene/MnO<sub>2</sub> nanotube hybrid structure by ultrafiltration technique [99\*] (Fig. 6a–c). The resultant hybrid structure possessed a large surface area for lithium-ion storage and maintained a good electrical conductivity. Lithium-ion batteries based on the layer-by-layer assembled graphene/MnO<sub>2</sub> anode exhibited a reversible capacity of 686 mAh/g at a current rate of 100 mA/g and 208 mAh/g at a high current rate of 1600 mA/g (Fig. 6d and e). On the other hand, Qiu et al. synthesized 3D graphene aerogel/TiO<sub>2</sub> hybrids by in-situ growth of TiO<sub>2</sub> single nanocrystals on the graphene surface using one-step hydrothermal method [103]. The lithium-ion batteries based on this hybrid structure delivered first discharge capacitance of 956.2 mAh/g and possessed an excellent capacity of 200 mAh/g after 50 cycles. The high rate capability of these 3D graphene composites based lithium ion batteries could be ascribed to the excellent conductivity and porosity of the 3D graphene.

Sn and Si can also be loaded on the 3D graphene surface and used as anode materials for lithium ion batteries. Specifically, Wang et al. synthesized 3D graphene/Sn architecture by mixing graphene oxide nanosheets dispersion with SnCl<sub>2</sub> aqueous solution, followed by a simultaneous reduction of GO and Sn<sup>+</sup> into graphene and Sn nanoparticle, respectively [101]. Lithium ion batteries based on the 3D graphene/Sn nanocomposite exhibited a highly reversible capacity of 795 mAh/g in the second cycle and 508 mAh/g in the 100th cycle.

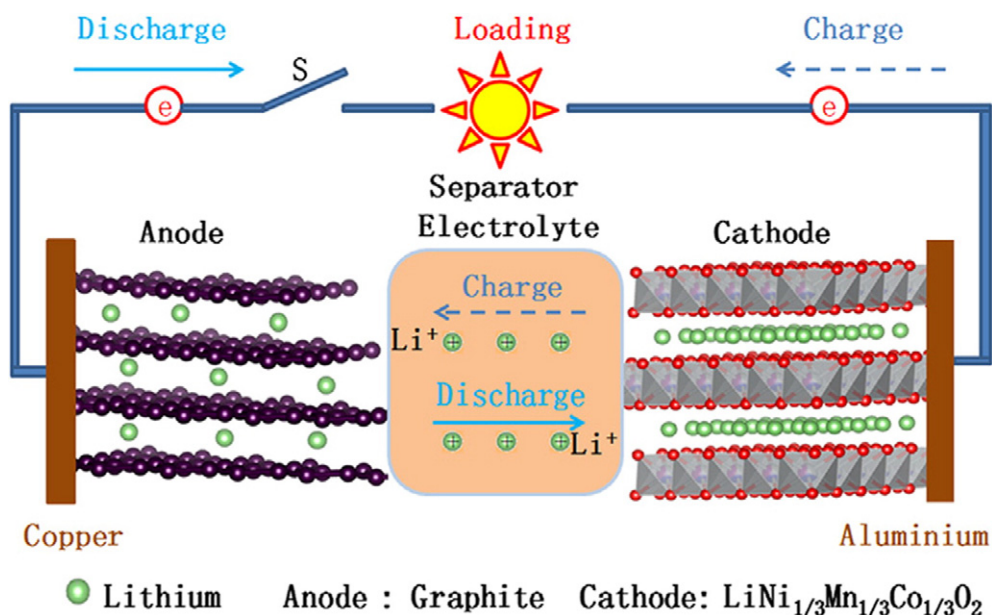


Fig. 5. Schematic illustration of typical lithium ion batteries. [93] (Reprinted from Ref. [93] with permission. Copyright 2013, Elsevier Ltd.).

Recently, Xu et al. fabricated lithium ion batteries with longer life and better stability. They fabricated the halogenated graphene nanoplatelets (XGNPs, X = Cl, Br, or I) by ball-milling graphite with chlorine ( $\text{Cl}_2$ ), bromine ( $\text{Br}_2$ ) or iodine ( $\text{I}_2$ ) [69] (Fig. 7a–e). The obtained IGnP possessed a high specific surface area of  $736.8 \text{ m}^2/\text{g}$ . The IGnP based lithium ion batteries exhibited the initial charge capacity of  $562.8 \text{ mAh/g}$ , and  $458.0 \text{ mAh/g}$  after 500 cycles. Furthermore, IGnP anode showed an

excellent stability as it still maintained a reversible capacity of  $464.1 \text{ mAh/g}$  for 100 cycles after 1 month storage at ambient condition ( $25^\circ \text{C}$ ) (Fig. 7f–h).

### 3.2.2. Cathode

The commonly used cathode materials based on lithium-transition metal oxide have a relatively low electrical conductivity, which limits

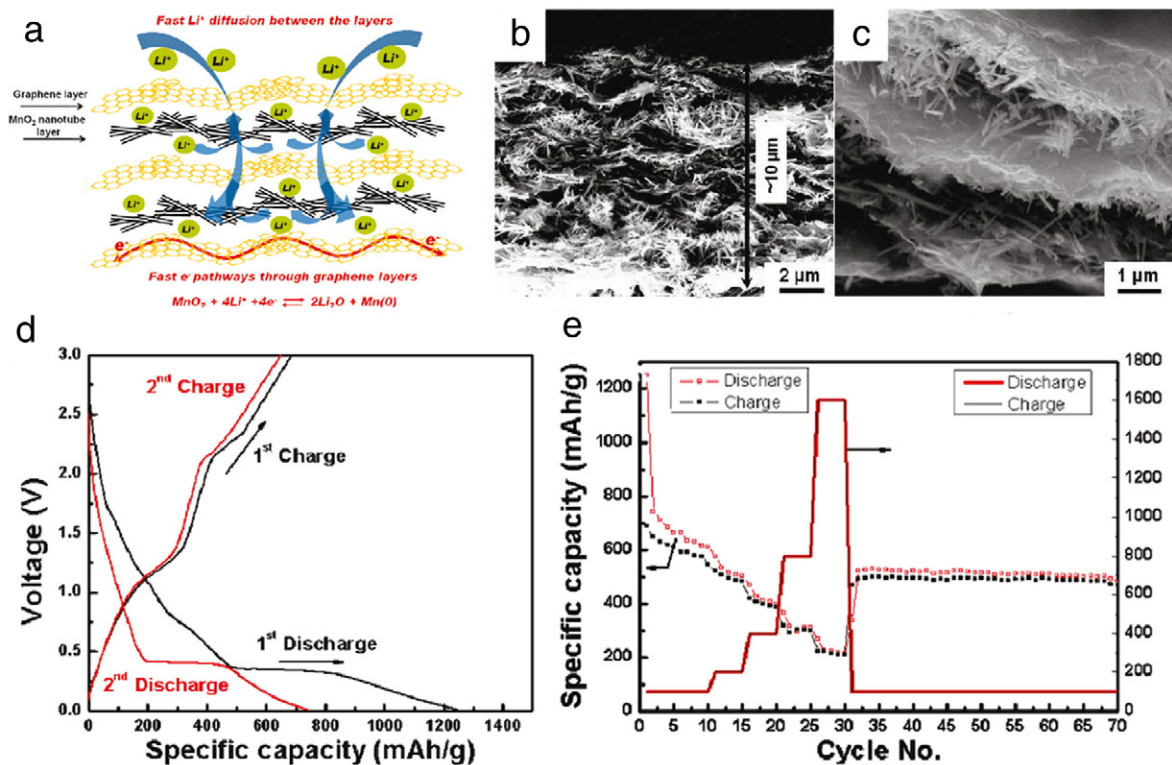
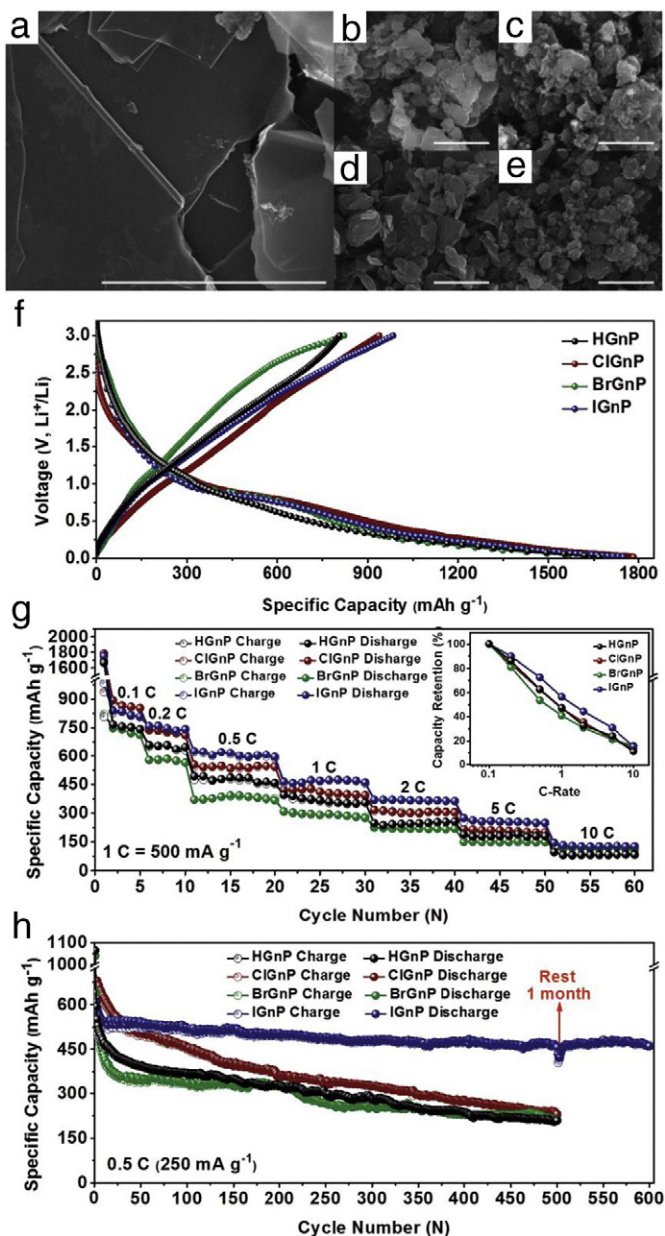


Fig. 6. (a) Schematic illustration of the layer-by-layer graphene/ $\text{MnO}_2$  nanotube structure. (b–c) SEM images of graphene/ $\text{MnO}_2$  film. (d) Galvanostatic charge and discharge curves, and (e) capacity at various current rates from  $100$  to  $1600 \text{ mA g}^{-1}$  with respect to the cycle number of the battery. [99] (Reprinted from Ref. [99] with permission. Copyright 2011, American Chemical Society).



**Fig. 7.** SEM images of (a) the pristine graphite; (b) HGnP; (c) ClGnP; (d) BrGnP; (e) IGnP. The scale bars are 1  $\mu\text{m}$ . (f) Initial discharge-charge profiles at 0.1 C; (g) rate performance. Inset charge capacity retention at different current densities; (h) cycling performance of HGnP and XGnPs (X = Cl, Br or I) in the voltage range of 0.02–3.0 V of the battery. [69] (Reprinted from Ref. [69] with permission. Copyright 2014, John Wiley & Sons, Inc.).

the performance of the lithium-ion batteries. Composites containing 3D graphene have been developed to improve the conductivity for enhancing the electrochemical properties of the cathode. Examples include spinel  $\text{LiMn}_2\text{O}_4$ /graphene hybrid [104],  $\text{LiFePO}_4$ /graphene [105],  $\text{LiMn}_{1-x}\text{Fe}_x\text{PO}_4$  nanorod/graphene [106], and  $\text{Li}_3\text{V}_2(\text{PO}_4)_3$  nanoparticle/graphene network [107,108]. Wang et al. synthesized  $\text{LiMn}_{1-x}\text{Fe}_x\text{PO}_4$  nanorod on rGO sheet by two-step approaches [106]. Fe-doped  $\text{Mn}_3\text{O}_4$  nanoparticles were grown on GO by controlled hydrolysis, followed by a reaction with Li and phosphate ions to form  $\text{LiMn}_{1-x}\text{Fe}_x\text{PO}_4$  nanorods on the surface of rGO. The lithium ion batteries based on the hybrid  $\text{LiMn}_{1-x}\text{Fe}_x\text{PO}_4$  nanorod/graphene exhibited stable capacities of 132 mAh/g and 107 mAh/g at high discharge rate of 20C and 50C, respectively. Similar with anode, the high rate capability also could be ascribed to the excellent conductivity and porous structure of the 3D graphene substrate.

Graphene foams produced by CVD method were also used to fabricate cathode as they have a relatively higher conductivity due to less defects. Ji et al. reported the use of 3D interconnected graphene foam/ $\text{LiFePO}_4$  as a cathode in a lithium ion battery by drop casting process [109]. This device delivered a specific capacity of 70 mAh/g at a high charge/discharge rate and a maximum specific capacity of 102 mAh/g, which was ~23% higher than that of the Al/ $\text{LiFePO}_4$  cathode and 170% higher than that of the Ni foam/ $\text{LiFePO}_4$  cathode because graphene interacted better with  $\text{LiFePO}_4$  than Al or Ni. In another study, Li and coworkers loaded  $\text{Li}_4\text{Ti}_5\text{O}_{12}$  and  $\text{LiFePO}_4$  onto the 3D graphene foams as anode and cathode, respectively [27]. These authors found that  $\text{Li}_4\text{Ti}_5\text{O}_{12}$ /graphene foam based lithium-ion batteries showed a high capacity of 170 mAh/g and retained a specific capacity of 135 mAh/g at a high charge/discharge rate.

### 3.3. Other batteries

Considering the high cost of lithium, sodium-ion batteries are an alternative energy storage device. Compared to graphite with relatively narrow interlayer distance, graphene becomes a good candidate as an active anode for sodium-ion batteries in view of the relatively larger sodium ionic radius in respect with that of lithium [78]. Indeed, Xu et al. reported the synthesis of nitrogen doped graphene foam as anode to significantly improve the performance of sodium-ion batteries [28]. In this case, large-size sodium-ions can access through the mesoporous network while the storage of sodium-ions can be improved. The nitrogen doped graphene foam based sodium-ion batteries exhibited an extremely high initial reversible capacity of 852.6 mAh/g at a current density of 500 mA/g and retained a charge capacity of 594 mAh/g even after 150 cycles. Lithium-air batteries are also one of the most promising energy storage devices with a theoretical energy density almost 10 times that of conventional lithium-ion batteries [110]. Xiao et al. reported a lithium-air batteries based on porous functionalized graphene air electrode [111]. Due to the unique bimodal porous structure,  $\text{O}_2$  can diffuse rapidly while high density of reactive sites for Li- $\text{O}_2$  reaction can be provided. As a consequence, the porous functionalized graphene based lithium-air batteries exhibited an exceptionally high capacity of 15,000 mAh/g.

## 4. Concluding remarks

As can be seen from above, much progress has been made in the development of 3D graphene electrode materials and various synthesis methods have been reported with both bottom-up and top-down approaches. 3D graphene, either grown on the catalyst substrate or reduced from graphene oxide, possesses a large surface area, high electrical conductivity, and good electrochemical stability. In conjunction with various other materials, including, but not limited to, metal/metal oxides, polymers, carbon allotropes, the 3D graphene based composites are promising electrode materials for high-performance supercapacitors and lithium ion batteries. However, there are still various challenges in fabricating perfect 3D graphene materials for practical applications in energy storage devices. First, the efficient surface area is still limited due to difficulties to precisely tune and control the porosity and structure in the 3D graphene architecture during the synthesis, and hence the obtained specific surface area is much lower than the theoretical value. Second, the electrical conductivity is high, but far lower than theoretical conductivity of ideal single layer graphene. Especially for the 3D graphene reduced from graphene oxide, the conductivity is seriously limited by the degree of reduction. For the 3D graphene grown by CVD, there is strong dependence of the quality and structure on the template and the synthesis temperature. Third, the ion and electron diffusion in the intrinsic microstructure should be further investigated to further improve electrochemical performance. Last, 3D graphene-based energy storage devices should be endowed with more functions, such as flexibility, stretchability, and wearability, to improve their practical

application value, particularly in wearable systems. Therefore, it is highly desirable to develop low-cost, eco-friendly innovative approaches to 3D graphene nanomaterials with tailor-made porous structures of controllable pore sizes. Besides, the electrical conductivity of 3D graphene materials needs to be further improved in compared with the ideal single-layer graphene of extremely high conductivity. With the continuing research efforts in developing 3D graphene nanomaterials, there will be continuous breakthroughs in the development of the 3D graphene based energy storage devices.

## References

- [1] Dai LM, Chang DW, Baek JB, Lu W. Carbon nanomaterials for advanced energy conversion and storage. *Small* 2012;8:1130–66.
- [2] Bonaccorso F, Colombo L, Yu GH, Stoller M, Tozzini V, Ferrari AC, et al. Graphene, related two-dimensional crystals, and hybrid systems for energy conversion and storage. *Science* 2015;347:1246501–11.
- [3] Geim AK, Novoselov KS. The rise of graphene. *Nat Mater* 2007;6:183–91.
- [4] Geim AK. Graphene: status and prospects. *Science* 2009;324:1530–4.
- [5] Novoselov KS, Geim AK, Morozov SV, Jiang D, Zhang Y, Dubonos SV, et al. Electric field effect in atomically thin carbon films. *Science* 2004;306:666–9. The single atom-thick sheets of carbon were first isolated and reported in this article
- [6] Allen MJ, Tung VC, Kaner RB. Honeycomb carbon: a review of graphene. *Chem Rev* 2010;110:132–45.
- [7] Novoselov KS, Geim AK, Morozov SV, Jiang D, Katsnelson MI, Grigorieva IV, et al. Two-dimensional gas of massless Dirac fermions in graphene. *Nature* 2005;438:197–200.
- [8] Balandin AA, Ghosh S, Bao WZ, Calizo I, Teweldebrhan D, Miao F, et al. Superior thermal conductivity of single-layer graphene. *Nano Lett* 2008;8:902–7.
- [9] Lee C, Wei XD, Kysar JW, Hone J. Measurement of the elastic properties and intrinsic strength of monolayer graphene. *Science* 2008;321:385–8.
- [10] Emtsev KV, Bostwick A, Horn K, Jobst J, Kellogg GL, Ley L, et al. Towards wafer-size graphene layers by atmospheric pressure graphitization of silicon carbide. *Nat Mater* 2009;8:203–7.
- [11] Sutter PW, Flege JI, Sutter EA. Epitaxial graphene on ruthenium. *Nat Mater* 2008;7:406–11.
- [12] Kim KS, Zhao Y, Jang H, Lee SY, Kim JM, Kim KS, et al. Large-scale pattern growth of graphene films for stretchable transparent electrodes. *Nature* 2009;457:706–10.
- [13] Reina A, Jia XT, Ho J, Nezich D, Son H, Bulovic V, et al. Large area, few-layer graphene films on arbitrary substrates by chemical vapor deposition. *Nano Lett* 2009;9:30–5.
- [14] Li XS, Cai WW, An JH, Kim S, Nah J, Yang DX, et al. Large-area synthesis of high-quality and uniform graphene films on copper foils. *Science* 2009;324:1312–4.
- [15] Park S, Ruoff RS. Chemical methods for the production of graphenes. *Nat Nanotechnol* 2009;4:217–24.
- [16] Hernandez Y, Nicolosi V, Lotya M, Blighe FM, Sun ZY, De S, et al. High-yield production of graphene by liquid-phase exfoliation of graphite. *Nat Nanotechnol* 2008;3:563–8.
- [17] Wu Q, Xu YX, Yao ZY, Liu AR, Shi GQ. Supercapacitors based on flexible graphene/polyaniline nanofiber composite films. *ACS Nano* 2010;4:1963–70.
- [18] Zhang LL, Zhou R, Zhao XS. Graphene-based materials as supercapacitor electrodes. *J Mater Chem* 2010;20:5983–92.
- [19] Wang GX, Shen XP, Yao J, Park J. Graphene nanosheets for enhanced lithium storage in lithium ion batteries. *Carbon* 2009;47:2049–53.
- [20] Yoo E, Kim J, Hosono E, Zhou HS, Kudo T, Honma I. Large reversible Li storage of graphene nanosheet families for use in rechargeable lithium ion batteries. *Nano Lett* 2008;8:2277–82.
- [21] Ma YF, Chen YS. Three-dimensional graphene networks: synthesis, properties and applications. *Nat Sci Rev* 2015;2:40–53.
- [22] Cao XH, Yin ZY, Zhang H. Three-dimensional graphene materials: preparation, structures and application in supercapacitors. *Energy Environ Sci* 2014;7:1850–65.
- [23] Chen ZP, Ren WC, Gao LB, Liu BL, Pei SF, Cheng HM. Three-dimensional flexible and conductive interconnected graphene networks grown by chemical vapour deposition. *Nat Mater* 2011;10:424–8. This article reports a template-directed CVD technique for the fabrication of macroscopic 3D graphene foam structures and provides the possibility to fabricate a broad class of 3D graphene of predetermined shapes.
- [24] Xu YX, Sheng KX, Li C, Shi GQ. Self-assembled graphene hydrogel via a one-step hydrothermal process. *ACS Nano* 2010;4:4324–30. This article reports the successful preparation of mechanically strong, electrically conductive, and thermally stable graphene hydrogel and provides a deeper understanding of the self-assembly behavior.
- [25] Du F, Yu DS, Dai LM, Ganguli S, Varshney V, Roy AK. Preparation of tunable 3D pillared carbon nanotube-graphene networks for high-performance capacitance. *Chem Mater* 2011;23:4810–6.
- [26] Xue Y, Ding Y, Niu JB, Xia ZH, Roy A, Chen H, et al. Rationally designed graphene-nanotube 3D architectures with a seamless nodal junction for efficient energy conversion and storage. *Sci Adv* 2015;1:1400198–206. This work realizes the seamlessly-bonded architecture through a one-step chemical vapor deposition in the first time and creates 3D graphene-CNT hollow fibers with radially aligned CNTs seamlessly sheathed by a cylindrical graphene layer.
- [27] Li N, Chen ZP, Ren WC, Li F, Cheng HM. Flexible graphene-based lithium ion batteries with ultrafast charge and discharge rates. *Proc Natl Acad Sci* 2012;109:17360–5.
- [28] Xu JT, Wang M, Wickramaratne NP, Jaroniec M, Dou SX, Dai LM. High-performance sodium ion batteries based on a 3D anode from nitrogen-doped graphene foams. *Adv Mater* 2015;27:2042–8.
- [29] He YM, Chen WJ, Li XD, Zhang ZX, Fu JC, Zhao CH, et al. Freestanding three-dimensional graphene/MnO<sub>2</sub> composite networks as ultralight and flexible supercapacitor electrodes. *ACS Nano* 2013;7:174–82.
- [30] Yoon JC, Lee JS, Kim SI, Kim KH, Jang JH. Three-dimensional graphene nanonetworks with high quality and mass production capability via precursor-assisted chemical vapor deposition. *Sci Rep* 2013;3:1788–95.
- [31] Ning GQ, Fan ZJ, Wang G, Gao JS, Qian WZ, Wei F. Gram-scale synthesis of nanomesh graphene with high surface area and its application in supercapacitor electrodes. *Chem Commun* 2011;47:5976–8.
- [32] Zhu Y, Zhang CG, Casillas G, Sun ZZ, Yan Z, Ruan GD, et al. A seamless three-dimensional carbon nanotube graphene hybrid material. *Nat Commun* 2012;3:1225–31.
- [33] Zhao Y, Liu J, Hu Y, Cheng HH, Hu CG, Jiang CC, et al. Highly compression-tolerant supercapacitor based on polypyrrole-mediated graphene foam electrodes. *Adv Mater* 2013;25:591–5. This work reports the rationally combined 3D graphene with PPy with a remarkable compression tolerance, and demonstrates the concept of compressible supercapacitor based on PPy-G foam for the first time.
- [34] Wu ZS, Winter A, Chen L, Sun Y, Turchanin A, Feng XL, et al. Three-dimensional nitrogen and boron co-doped graphene for high-performance all-solid-state supercapacitors. *Adv Mater* 2012;24:5130–5.
- [35] Chen WF, Li SR, Chen CH, Yan LF. Self-assembly and embedding of nanoparticles by in situ reduced graphene for preparation of a 3D graphene/nanoparticle aerogel. *Adv Mater* 2011;23:5679–83.
- [36] Choi BG, Yang M, Hong WH, Choi JW, Huh YS. 3D macroporous graphene frameworks for supercapacitors with high energy and power densities. *ACS Nano* 2012;6:4020–8.
- [37] Yang SY, Chang KH, Tien HW, Lee YF, Li SM, Wang YS, et al. Design and tailoring of a hierarchical graphene-carbon nanotube architecture for supercapacitors. *J Mater Chem* 2011;21:2374–80.
- [38] Xu YX, Lin ZY, Zhong X, Papandrea B, Huang Y, Duan XF. Solvated graphene frameworks as high-performance anodes for lithium-ion batteries. *Angew Chem Int Ed* 2015;54:5345–50.
- [39] Dresselhaus MS, Jorio A, Hofmann M, Dresselhaus G, Saito R. Perspectives on carbon nanotubes and graphene Raman spectroscopy. *Nano Lett* 2010;10:751–8.
- [40] Zhou M, Lin TQ, Huang FQ, Zhong YJ, Wang Z, Tang YF, et al. Highly conductive porous graphene/ceramic composites for heat transfer and thermal energy storage. *Adv Funct Mater* 2013;23:2263–9.
- [41] Wei W, Yang SB, Zhou HX, Lieberwirth I, Feng XL, Müllen K. 3D graphene foams cross-linked with pre-encapsulated Fe<sub>3</sub>O<sub>4</sub> nanospheres for enhanced lithium storage. *Adv Mater* 2013;25:2909–14.
- [42] Luo JS, Liu JL, Zeng ZY, Ng CF, Ma LJ, Zhang H, et al. Three-dimensional graphene foam supported Fe<sub>3</sub>O<sub>4</sub> lithium battery anodes with long cycle life and high rate capability. *Nano Lett* 2013;13:6136–43.
- [43] Dong XC, Xu H, Wang XW, Huang YX, Chan-Park MB, Zhang H, et al. 3D graphene-cobalt oxide electrode for high-performance supercapacitor and enzymeless glucose detection. *ACS Nano* 2012;6:3206–13.
- [44] Cao XH, Shi YM, Shi WH, Lu G, Huang X, Yan QY, et al. Preparation of novel 3D graphene networks for supercapacitor applications. *Small* 2011;7:3163–8. This work provides a new way to fabricate graphene-based composite materials and proves that graphene can be served as an ideal platform to construct 3D graphene/metal oxide composites.
- [45] Dong XC, Wang JX, Wang J, Chan-Park MB, Li XG, Wang LH, et al. Supercapacitor electrode based on three-dimensional graphene-polyaniline hybrid. *Mater Chem Phys* 2012;134:576–80.
- [46] Paraknowitsch JP, Thomas A. Doping carbons beyond nitrogen: an overview of advanced heteroatom doped carbons with boron, sulphur and phosphorus for energy applications. *Energy Environ Sci* 2013;6:2839–55.
- [47] Xue YH, Liu J, Chen H, Wang RG, Li DQ, Qu J, et al. Nitrogen-doped graphene foams as metal-free counter electrodes in high-performance dye-sensitized solar cells. *Angew Chem Int Ed* 2012;51:12124–7.
- [48] Xue YH, Yu DS, Dai LM, Wang RG, Li DQ, Roy A, et al. Three-dimensional B, N-doped graphene foam as a metal-free catalyst for oxygen reduction reaction. *Phys Chem Chem Phys* 2013;15:12220–6.
- [49] Sun ZZ, Yan Z, Yao J, Beitler E, Zhu Y, Tour JM. Growth of graphene from solid carbon sources. *Nature* 2010;468:549–52. This article demonstrated a one-step method for the controllable growth of both pristine graphene and doped graphene using solid carbon sources and offered a broad view to establish a 3D graphene structure by coating of solid carbon sources.
- [50] Shan CS, Tang H, Wong TL, He LF, Lee ST. Facile synthesis of a large quantity of graphene by chemical vapor deposition: an advanced catalyst carrier. *Adv Mater* 2012;24:2491–5.
- [51] Yang CY, Bin H, Wan DY, Huang FQ, Xie XM, Jiang MJ. Direct PECVD growth of vertically erected graphene walls on dielectric substrates as excellent multifunctional electrodes. *J Mater Chem A* 2013;1:770–5.
- [52] Xiao XC, Xie T, Cheng YT. Self-healable graphene polymer composites. *J Mater Chem* 2010;20:3508–14.
- [53] Dato A, Radmilovic V, Lee Z, Phillips J, Frenklach M. Substrate-free gas-phase synthesis of graphene sheets. *Nano Lett* 2008;8:2012–6.
- [54] Bai H, Li C, Wang XL, Shi GQ. On the gelation of graphene oxide. *J Phys Chem C* 2011;115:5545–51.

- [55] Hummers WS, Offeman RE. Preparation of graphitic oxide. *J Am Chem Soc* 1958;80:1339. Hummer's method to fabricate the graphene oxide have become a classic approach.
- [56] Li D, Muller MB, Gilje S, Kaner RB, Wallace GG. Processable aqueous dispersions of graphene nanosheets. *Nat Nanotechnol* 2008;3:101–5.
- [57] Li C, Shi GQ. Three-dimensional graphene architectures. *Nanoscale* 2012;4:5549–63.
- [58] Tang ZH, Shen SL, Zhuang J, Wang X. Noble-metal-promoted three-dimensional macroassembly of single-layered graphene oxide. *Angew Chem Int Ed* 2010;49:4603–7.
- [59] Chen WF, Yan LF. In situ self-assembly of mild chemical reduction graphene for three-dimensional architectures. *Nanoscale* 2011;3:3132–7.
- [60] Hu CG, Zhai XQ, Liu LL, Zhao Y, Jiang L, Qu LT. Spontaneous reduction and assembly of graphene oxide into three-dimensional graphene network on arbitrary conductive substrates. *Sci Rep* 2013;3:2065–74.
- [61] Liu F, Seo TS. A controllable self-assembly method for large-scale synthesis of graphene sponges and free-standing graphene films. *Adv Funct Mater* 2010;20:1930–6.
- [62] Bai H, Li C, Wang XL, Shi GQ. A pH-sensitive graphene oxide composite hydrogel. *Chem Commun* 2010;46:2376–8.
- [63] Xu YX, Wu QO, Sun YQ, Bai H, Shi GQ. Three-dimensional self-assembly of graphene oxide and DNA into multifunctional hydrogels. *ACS Nano* 2010;4:7358–62.
- [64] Zhang XT, Sui ZY, Xu B, Yue SF, Luo YJ, Zhan WC, et al. Mechanically strong and highly conductive graphene aerogel and its use as electrodes for electrochemical power sources. *J Mater Chem* 2011;21:6494–7.
- [65] Cong HP, Ren XC, Wang P, Yu SH. Macroscopic multifunctional graphene-based hydrogels and aerogels by a metal ion induced self-assembly process. *ACS Nano* 2012;6:2693–703.
- [66] Sheng KX, Sun YQ, Li C, Yuan WJ, Shi GQ. Ultrahigh-rate supercapacitors based on electrochemically reduced graphene oxide for AC line-filtering. *Sci Rep* 2012;2:247–51.
- [67] Xiao XY, Beechem TE, Brumbach MT, Lambert TN, Davis DJ, Michael JR, et al. Lithographically defined three-dimensional graphene structures. *ACS Nano* 2012;6:3573–9.
- [68] Lee SH, Kim HW, Hwang JO, Lee WJ, Kwon J, Bielawski CW, et al. Three-dimensional self-assembly of graphene oxide platelets into mechanically flexible macroporous carbon films. *Angew Chem Int Ed* 2010;49:10084–8.
- [69] Xu JT, Jeon IY, Seo JM, Dou SX, Dai LM, Baek JB. Edge-selectively halogenated graphene nanoplatelets (XGnPs, X = Cl, Br, or I) prepared by ball-milling and used as anode materials for lithium-ion batteries. *Adv Mater* 2014;26:7317–23. The first study on the use of edge-selectively halogenated GnPs (XGnPs, X = Cl, Br, or I) prepared by the low-cost and large scale production of ball-milling method as anode materials for LIBs.
- [70] Ning GQ, Xu CG, Cao YM, Zhu X, Jiang ZM, Fan ZJ, et al. Chemical vapor deposition derived flexible graphene paper and its application as high performance anodes for lithium rechargeable batteries. *J Mater Chem A* 2013;1:408–14.
- [71] Li X, Sun PZ, Fan LL, Zhu M, Wang KL, Zhong ML, et al. Multifunctional graphene woven fabrics. *Sci Rep* 2012;2:395–402.
- [72] Fan XL, Chen T, Dai LM. Graphene networks for high-performance flexible and transparent supercapacitors. *RSC Adv* 2014;4:36996–7002.
- [73] Paul RK, Ghazinejad M, Penchev M, Lin J, Ozkan M, Ozkan CS. Synthesis of a pillared graphene nanostructure: a counterpart of three-dimensional carbon architectures. *Small* 2010;6:2309–13.
- [74] You B, Wang LL, Yao L, Yang J. Three dimensional N-doped graphene-CNT networks for supercapacitor. *Chem Commun* 2013;49:5016–8.
- [75] Yu DS, Dai LM. Self-assembled graphene/carbon nanotube hybrid films for supercapacitors. *J Phys Chem Lett* 2010;1:467–70.
- [76] Lin J, Zhang CG, Yang Z, Zhu Y, Peng ZW, Hauge RH, et al. 3-Dimensional graphene carbon nanotube carpet-based microsupercapacitors with high electrochemical performance. *Nano Lett* 2013;13:72–8.
- [77] Fan ZJ, Yan J, Zhi LJ, Zhang Q, Wei T, Feng J, et al. A three-dimensional carbon nanotube/graphene sandwich and its application as electrode in supercapacitors. *Adv Mater* 2010;22:3723–8.
- [78] Winter M, Brodd RJ. What are batteries, fuel cells, and supercapacitors? *Chem Rev* 2004;104:4245–69.
- [79] Raccichini R, Varzi A, Passerini S, Scrosati B. The role of graphene for electrochemical energy storage. *Nat Mater* 2015;14:271–9.
- [80] Zhang LL, Zhao XS. Carbon-based materials as supercapacitor electrodes. *Chem Soc Rev* 2009;38:2520–31.
- [81] Simon P, Gogotsi Y. Materials for electrochemical capacitors. *Nat Mater* 2008;7:845–54. This article is a comprehensive review on the developments of materials, especially carbon nanotubes, for electrochemical capacitors.
- [82] Chen T, Dai LM. Carbon nanomaterials for high-performance supercapacitors. *Mater Today* 2013;16:272–80.
- [83] Novoselov KS, Fal'ko VI, Colombo L, Gellert PR, Schwab MG, Kim K. A roadmap for graphene. *Nature* 2012;490:192–200.
- [84] Yu XZ, Lu BA, Xu Z. Super long-life supercapacitors based on the construction of nanohoneycomb-like strongly coupled CoMoO<sub>4</sub>-3D graphene hybrid electrodes. *Adv Mater* 2014;26:1044–51.
- [85] Gong YJ, Yang SB, Liu Z, Ma LL, Vajtai R, Ajayan PM. Graphene-network-backboned architectures for high-performance lithium storage. *Adv Mater* 2013;25:3979–84.
- [86] Zhang L, Shi GQ. Preparation of highly conductive graphene hydrogels for fabricating supercapacitors with high rate capability. *J Phys Chem C* 2011;115:17206–12.
- [87] Xu YX, Lin ZY, Huang XQ, Liu Y, Huang Y, Duan XF. Flexible solid-state supercapacitors based on three-dimensional graphene hydrogel films. *ACS Nano* 2013;7:4042–9.
- [88] Ye SB, Feng JC. Self-assembled three-dimensional hierarchical graphene/polypyrrole nanotube hybrid aerogel and its application for supercapacitors. *ACS Appl Mater Interfaces* 2014;6:9671–9.
- [89] Wu ZS, Sun Y, Tan YZ, Yang SB, Feng XL, Müllen K. Three-dimensional graphene-based macro- and mesoporous frameworks for high-performance electrochemical capacitive energy storage. *J Am Chem Soc* 2012;134:19532–5.
- [90] Yan J, Fan ZJ, Wei T, Qian WZ, Zhang ML, Wei F. Fast and reversible surface redox reaction of graphene-MnO<sub>2</sub> composites as supercapacitor electrodes. *Carbon* 2010;48:3825–33.
- [91] Chen S, Zhu JW, Wu XD, Han QF, Wang X. Graphene oxide-MnO<sub>2</sub> nanocomposites for supercapacitors. *ACS Nano* 2010;4:2822–30.
- [92] Bruce PG, Scrosati B, Tarascon JM. Nanomaterials for rechargeable lithium batteries. *Angew Chem Int Ed* 2008;47:2930–46.
- [93] Xu JT, Dou SX, Liu HK, Dai LM. Cathode materials for next generation lithium ion batteries. *Nano Energy* 2013;2:439–42.
- [94] Liu F, Song SY, Xue DF, Zhang HJ. Folded structured graphene paper for high performance electrode materials. *Adv Mater* 2012;24:1089–94.
- [95] Abouimrane A, Compton OC, Amine K, Nguyen ST. Non-annealed graphene paper as a binder-free anode for lithium-ion batteries. *J Phys Chem C* 2010;114:12800–4.
- [96] Li L, Zhou GM, Weng Z, Shan XY, Feng Li, Cheng HM. Monolithic Fe<sub>2</sub>O<sub>3</sub>/graphene hybrid for highly efficient lithium storage and arsenic removal. *Carbon* 2014;67:500–7.
- [97] Wang RH, Xu CH, Sun J, Gao L, Lin CC. Flexible free-standing hollow Fe<sub>3</sub>O<sub>4</sub>/graphene hybrid films for lithium-ion batteries. *J Mater Chem A* 2013;1:1794–800.
- [98] Shen LF, Zhang XG, Li HS, Yuan CZ, Cao GZ. Design and tailoring of a three-dimensional TiO<sub>2</sub>-graphene-carbon nanotube nanocomposite for fast lithium storage. *J Phys Chem Lett* 2011;2:3096–101.
- [99] Yu AP, Park HW, Davies A, Higgins DC, Chen ZW, Xiao XC. Free-standing layer-by-layer hybrid thin film of graphene-MnO<sub>2</sub> nanotube as anode for lithium ion batteries. *J Phys Chem Lett* 2011;2:1855–60. This work reported an ultrathin, free-standing and layer-by-layer assembled graphene-MnO<sub>2</sub> nanotube film with a unique nanostructure as an anode material, which achieved a high performance in Li ion batteries.
- [100] Wang HL, Cui LF, Yang Y, Casaloung HS, Robinson JT, Liang YY, et al. Mn<sub>3</sub>O<sub>4</sub>-graphene hybrid as a high-capacity anode material for lithium ion batteries. *J Am Chem Soc* 2010;132:13978–80.
- [101] Wang GX, Wang B, Wang XL, Park J, Dou SX, Ahn H, et al. Sn/graphene nanocomposite with 3D architecture for enhanced reversible lithium storage in lithium ion batteries. *J Mater Chem* 2009;19:8378–84.
- [102] Lee JK, Smith KB, Hayner M, Kung HH. Silicon nanoparticles-graphene paper composites for Li ion battery anodes. *Chem Commun* 2010;46:2025–7.
- [103] Qiu BC, Xing MY, Zhang JL. Mesoporous TiO<sub>2</sub> nanocrystals grown in situ on graphene aerogels for high photocatalysis and lithium-ion batteries. *J Am Chem Soc* 2014;136:5852–5.
- [104] Bak SM, Nam KW, Lee CW, Kim KH, Jung HC, Yang XQ, et al. Spinel LiMn<sub>2</sub>O<sub>4</sub>/reduced graphene oxide hybrid for high rate lithium ion batteries. *J Mater Chem* 2011;21:17309–15.
- [105] Yang JL, Wang JJ, Wang DN, Lia XF, Geng DS, Liang GX, et al. 3D Porous LiFePO<sub>4</sub>/graphene hybrid cathodes with enhanced performance for Li-ion batteries. *J Power Sources* 2012;208:340–4.
- [106] Wang HL, Yang Y, Liang YY, Cui LF, Casaloung HS, Li YG, et al. LiMn<sub>1-x</sub>Fe<sub>x</sub>PO<sub>4</sub> nanorods grown on graphene sheets for ultrahigh-rate-performance lithium ion batteries. *Angew Chem Int Ed* 2011;50:7364–8.
- [107] Jiang Y, Xu WW, Chen DD, Jiao Z, Zhang HJ, Ma QL, et al. Graphene modified Li<sub>3</sub>V<sub>2</sub>(PO<sub>4</sub>)<sub>3</sub> as a high-performance cathode material for lithium ion batteries. *Electrochim Acta* 2012;85:377–83.
- [108] Rui XH, Sim DH, Wong KM, Zhu JX, Liu WL, Xu C, et al. Li<sub>3</sub>V<sub>2</sub>(PO<sub>4</sub>)<sub>3</sub> nanocrystals embedded in ananoporous carbon matrix supported on reduced graphene oxide sheets: binder-free and high rate cathode material for lithium-ion batteries. *J Power Sources* 2012;214:171–7.
- [109] Ji HX, Zhang LL, Pettes MT, Li HF, Chen SS, Shi L, et al. Ultrathin graphite foam: a three-dimensional conductive network for battery electrodes. *Nano Lett* 2012;5:2446–51.
- [110] Bruce PG, Freunberger SA, Hardwick LJ, Tarascon JM. Li–O<sub>2</sub> and Li–S batteries with high energy storage. *Nat Mater* 2012;11:19–29.
- [111] Xiao J, Mei D, Li X, Xu W, Wang D, Graff GL, et al. Hierarchically porous graphene as a lithium-air battery electrode. *Nano Lett* 2011;11:5071–8.